Photosynthetic Light Reactions in Diatoms. I. The Lipids and Light-Harvesting Complexes of the Thylakoid Membrane

Claudia Büchel, Reimund Goss, Benjamin Bailleul, Douglas Campbell, Johann Lavaud, Bernard Lepetit

Chapter 1: Photosynthetic light reactions in diatoms. I. The lipids and light-harvesting complexes of the thylakoid membrane

Claudia Büchel[1*], Reimund Goss[2*], Benjamin Bailleul[3], Douglas A. Campbell[4], Johann Lavaud[5,6], Bernard Lepetit[7]

* equal contribution

1 Institute of Molecular Biosciences, Goethe University Frankfurt, 60438 Frankfurt, Germany
2 Institute of Biology, Leipzig University, 04103 Leipzig, Germany
3 Laboratoire de Biologie du Chloroplaste et Perception de la Lumière chez les Micro-algues, UMR7141, IBPC, CNRS- Sorbonne Université, Paris, France
4 Department of Biology, Mount Allison University, NB, Canada
5 UMI3376 Takuvik, CNRS/ULaval, Département de Biologie, Université Laval, Pavillon Alexandre-Vachon, 1045 avenue de la Médecine, Québec (Qc) G1V0A6, Canada
6 Present address: UMR6539 LEMAR, CNRS/Univ Brest/Ifremer/IRD, Institut Européen de la Mer, Technopôle Brest-Iroise, rue Dumont d'Urville, 29280 Plouzané, France
7 Plant Ecophysiology, Department of Biology, University of Konstanz, 78457 Konstanz, Germany

Correspondences: c.buechel@bio.uni-frankfurt.de; rgoss@rz.uni-leipzig.de

Abstract

Light harvesting and photochemistry is performed by photosystems coupled to specific antennae embedded in the thylakoid membrane, a common principle across diatoms, plants and green algae. Still, unique features of diatoms within this common principle have been unraveled in recent decades, likely resulting from the complex evolutionary history of diatoms. These unique features are found in (i) the lipid composition of the thylakoid membrane, ii) the spatial organization of the light harvesting complexes, and iii) their protein and pigment composition. This chapter summarizes current knowledge of these three specific features, with a focus on structural and functional properties.

Key words: diatoms, FCP, LHC, light harvesting, lipids, thylakoids, xanthophyll cycle

Table of content

p4: Introduction

p6: 1. Thylakoid lipids

p6: 1.1 The lipid composition of thylakoid membranes

p8: 1.2 Fatty acid composition of thylakoid membrane lipids

p9: 1.3 Function of thylakoid membrane lipids

p11: 1.4 Localization of thylakoid membrane lipids

p13: 2. Light harvesting

p13: 2.1 The diatom light harvesting systems

p14: 2.2 Subunit compositions of light harvesting complexes

p15: 2.3 FCPs associated with PSI

p16: 2.4 FCPs associated with PSII

p18: 2.5 Molecular structure of FCPs

p20: 2.6 Excitation energy transfer in FCPs

p23: Outlook

p24: References

p31: Acknowledgements

Abbreviations

C. meneghiniana: Cyclotella meneghiniana
Ch. gracilis: Chaetoceros gracilis
Chl: chlorophyll
Dd: diadinoxanthin
DGDG: digalactosyldiacylglycerol
DGGC: diacylglycerylcarboxyhydroxymethylcholine
DGTA: diacylglycerylhydroxymethyl-N,N,N-trimethyl-β-alanine
DGTS: diacylgyceryl-N-trimethylhomoserine
DHA: docosahexaenoic acid
Dt: diatoxanthin
EPA: eicosapentaenoic acid
FCP: fucoxanthin-chlorophyll-protein complex
Fx: fucoxanthin
H_{II}: inverted hexagonal phase
H. ostrearia: Haslea ostrearia
ICT: intramolecular charge transfer
LHC: light-harvesting complex
MGDG: monogalactosyldiacylglycerol
P. tricornutum: Phaeodactylum tricornutum
PG: phosphatidylglycerol
PSI: photosystem I
PSII: photosystem II
PUFAs: polyunsaturated fatty acids
qE: energy dependent quenching
SQDG: sulphoquinovosyldiacylglycerol
T. pseudonana: Thalassiosira pseudonana
XC: xanthophyll cycle

Introduction

Diatoms perform oxygenic photosynthesis, whereby the basic reactions are identical in all eukaryotes: light energy is absorbed by the pigments bound to photosystem (PS) I and II and their associated light-harvesting complexes (LHC). It is transferred to special chlorophyll (Chl) *a* molecules in the PS, the so-called reaction center Chls, where charge separation takes place. This fuels the photosynthetic electron transport, where electrons are subtracted from water and eventually used for the generation of NADPH (Fig. 1A). These photosynthetic light reactions take place in the thylakoid membranes, and the coupling of the electron transfer to a unidirectional transport of protons leads to accumulation of protons in the lumen that is used by an ATP-Synthase to generate ATP (for details see "*Photosynthetic light reactions in diatoms. II. The dynamic regulation of the various light reactions*"). NADPH and ATP are then mainly used by the Calvin cycle in the chloroplast stroma to fix CO_2. Thus, diatoms share the same elementary photosynthetic modules with other organisms performing oxygenic photosynthesis (Falkowski et al. 2008), which are fairly similar in all eukaryotes, with one exception: Light-harvesting systems differ significantly amongst the different taxa (Neilson and Durnford 2010, Büchel 2015, Büchel 2020, Croce and van Amerongen, 2020). In addition, there are further subtle changes concerning photosystems and their functional organization. For example, the PSII core recently crystallized from *Chaetoceros gracilis* contains four more Chl *a* molecules than the plant PSII core, and one additional subunit shielding the oxygen evolving complex (Nagao et al. 2019a). With more than 100,000 species of diatoms present on earth, exhibiting a huge phylogenetic diversity (Mann and Vanormelingen 2013), we may also assume some diversity among diatom species even within these elementary modules.

The photosynthetic modules are embedded in the thylakoid membrane. In contrast to the green lineage, diatom thylakoids are organized in homogeneous stacks of three which run along the whole diatom plastid (Berkaloff et al. 1990) (Fig. 1B). They do not show the grana stroma differentiation which imposes the lateral segregation of the PSII and PSI in plants (Anderson 1999). In diatoms, immunolocalization studies, lipid analyses, and 3D reconstruction showed that PSI are mostly found in the stroma-facing external thylakoids whereas PSII are embedded in the core of the stack, at the interface of two thylakoids (Pyszniak and Gibbs 1992; Lepetit et al. 2012; Flori et al. 2017). This heterogeneity is enforced under red light conditions, which induce an unusual stacking of diatom thylakoids. Here, large areas were revealed which are exclusively occupied by PSI supercomplexes consisting of PSI cores with their PSI-specific antenna of Lhcr proteins (Bína et al. 2016). In line with this, clusters of PSII cores including their FCP antennae have been revealed by cryo-electron tomography in *Phaeodactylum*

tricornutum recently (Levitan et al. 2019). For steric reasons the ATP synthase is located in the outer thylakoids. The vicinity of PSII and PSI, as well as some connections between thylakoids, ensures a fast diffusion of electron shuttles between the two photosystems (Flori et al. 2017), whereas their diffusion can limit the overall rate of the linear electron flow in plants (Kirchhoff et al. 2004; Kirchhoff et al. 2011). This peculiar segregation also has important consequences for the regulation of the light capture by the two photosystems, by preventing the share of excitons between them (Flori et al. 2017), a process found in cyanobacteria and red algae, and called spillover (Biggins and Bruce 1989). Whether based on immunoblot quantification or functional measurements, diatoms seem to possess more PSII than PSI, in contrast to plants and green algae where PSI occurs at least in the same amount as PSII (Smith and Melis 1988; Strzepek and Harrison 2004; Thamatrakoln et al. 2013). With this higher amount of PSII, diatoms may compensate their slightly lower maximum PSII efficiency, which is usually around 0.6-0.7, while in plants it reaches values of ~0.84 (Kalaji et al. 2014).

Lipids and pigmented proteins are the major components of the diatom thylakoid membrane. Usually, the proteins occupy an area of 70-80 % of the thylakoid membrane, while lipids correspondingly contribute to 20-30 % (Kirchhoff 2014). Compared to the green lineage, both the respective amounts of the different thylakoid lipid classes and the respective fatty acids composition is considerably different in diatoms. Moreover, the structure and composition of the light harvesting system, the dominant protein constituent of the thylakoid membranes, shows various diatom specific peculiarities. Certainly one reason for these differences is based on the complex evolutionary history of diatoms - with plastids originating from secondary endosymbiosis with red algae, while considerable amounts of ‘green’ genes are also found in the diatom genome (Dorrell et al. 2017).

In this review article, we will summarize current knowledge on lipid composition (part 1) and antennae structures of diatom thylakoids (part 2).

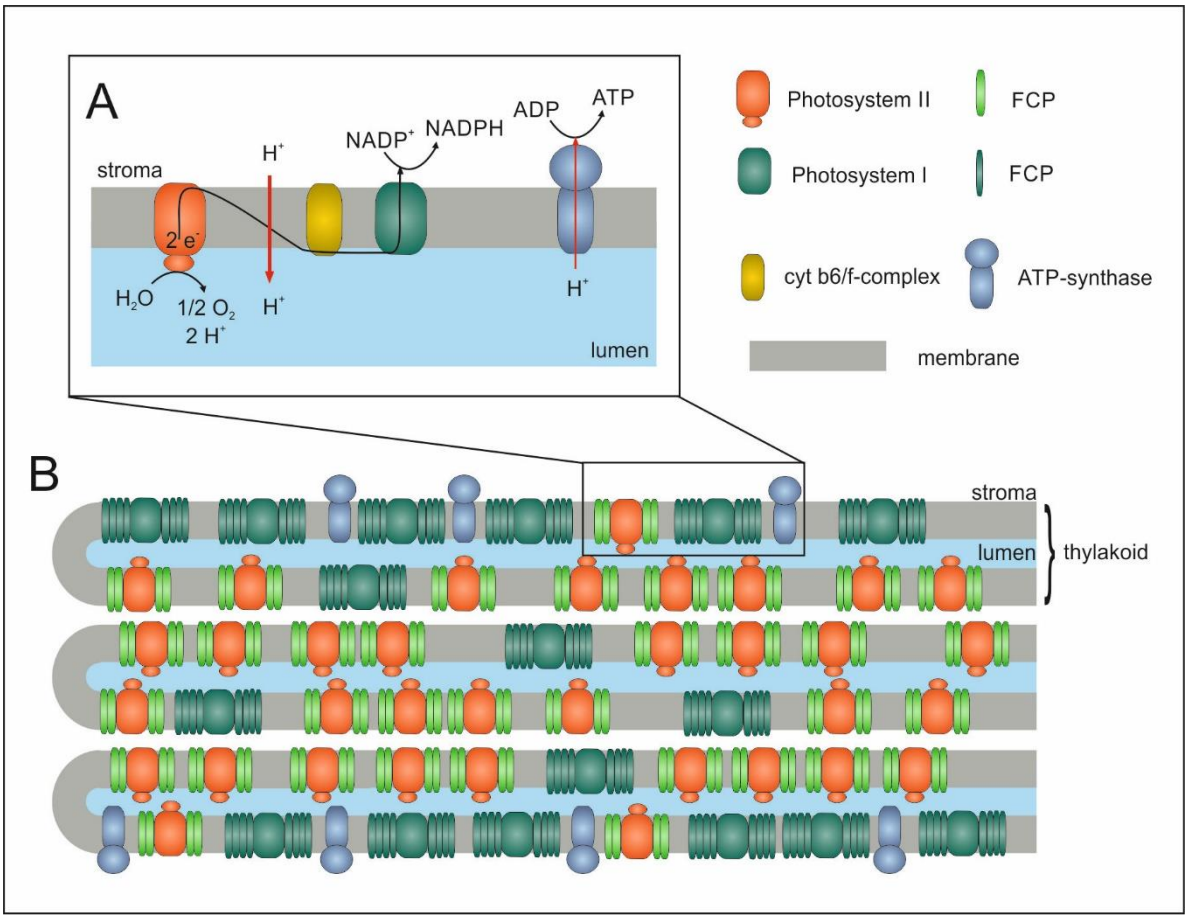

Figure 1: (A) General, simplified scheme of the light reactions of photosynthesis. Only PSII (red) cytb6/f complex (yellow), PSI (green) and ATPsynthase (blue) are shown. Light-harvesting systems have been omitted since they differ significantly between the different algal groups and higher plants. For more detail on electron and proton transfer refer to Figure 1 in chapter "*Photosynthetic light reactions in diatoms. II. The dynamic regulation of the various light reactions"*. (B) Scheme of the thylakoid membrane structure of diatoms (B). The thylakoids are organized in stacks of three that span the whole plastid. The outer membranes of such stack are enriched in PSI, whereas PSII is predominantly found in the inner four membranes. Cytb6/f complexes that are not preferentially localized (Flori et al. 2017) have been omitted as well as connections between thylakoids of one stack. In diatoms the light-harvesting complexes are called fucoxanthin-chlorophyll proteins (FCP). FCPs tightly bound to PSII are shown in light green, FCPs belonging to PSI are shown in dark green.

1. Thylakoid lipids

1.1 The lipid composition of thylakoid membranes

Before the lipid and fatty acid composition of diatom thylakoid membranes is presented in detail, it should be mentioned that most of the depicted results have been derived from laboratory experiments under defined growth conditions (for details please refer to the cited references). However, in their natural environment diatoms are exposed to extreme differences

in temperature and light intensities. To cope with these extreme abiotic conditions diatoms adjust the lipid and fatty acid composition of the thylakoids in order to maintain the membrane in a fluid working state (see also 1.2 and 1.3).

The diatom thylakoid membranes are composed of the two neutral galactolipids monogalactosyldiacylglycerol (MGDG) and digalactosyldiacylglycerol (DGDG), the negatively charged sulfolipid sulphoquinovosyldiacylglycerol (SQDG) and the anionic phospholipid phosphatidylglycerol (PG) (Vieler et al. 2007; Goss et al. 2009; Lepetit et al. 2012; Abida et al. 2015). These lipids are also found in higher plants, but in addition the diatom thylakoid membranes can contain low amounts of betaine lipids like diacylglycerylcarboxyhydroxymethylcholine (DGGC) and diacylglycerylhydroxymethyl-N,N,N-trimethyl-β-alanine (DGTA) (Vieler et al. 2007; Canavate et al. 2016). A third betaine lipid, namely diacylgyceryl-N-trimethylhomoserine (DGTS), which acts as precursor in the synthesis of DGTA, can be found in trace amounts (Canavate et al. 2016). Phosphatidylcholine, which in higher plant thylakoid preparations is supposed to represent a contamination with chloroplast envelope membranes, seems to be a general constituent of diatom thylakoid membranes (Vieler et al. 2007; Goss et al. 2009; Lepetit et al. 2012).

Although the main lipids of diatom thylakoids are comparable to those of the green lineage, their contribution to the overall lipid content of the membrane is significantly different. While in higher plants and green algae the neutral galactolipids dominate the lipid content of the thylakoid membrane and amount to 70 to 80% of the total lipid (Murata and Siegenthaler 1998), the concentrations of MGDG and DGDG are strongly reduced in the thylakoids of pennate (*P. tricornutum*) and centric (*Cyclotella meneghiniana*) diatoms (Goss et al. 2009; Lepetit et al. 2012; Abida et al. 2015). The reduction of MGDG and DGDG is accompanied by simultaneous increases of the two negatively charged lipids SQDG and PG. This is especially obvious in thylakoid membranes of *P. tricornutum* or *C. meneghiniana* purified from high light grown cultures (Lepetit et al. 2012). They contain SQDG as the most abundant lipid, and the combined negatively charged lipids SQDG and PG contribute to more than 50% of the total thylakoid lipids. The ratio of neutral to negatively charged lipids lies between one and two and is thus significantly lower than the typical values between three and four observed in higher plant and green algal thylakoid membranes. High concentrations of the negatively charged lipids SQDG and PG in diatom thylakoid membranes are supported by the study of Yan et al. (2011) who determined the photosynthetic lipid and fatty acid profile of three different strains of the marine diatom *Skeletonema* sp.. Two of the three strains show high SQDG concentrations (35-40% of

the photosynthetic lipids) and, in combination with PG, the negatively charged lipids amount to almost 50% of the total photosynthetic lipids of *Skeletonema*.

1.2 Fatty acid composition of thylakoid membrane lipids

Diatoms are characterized by the synthesis of very long-chain polyunsaturated fatty acids (PUFAs) with chain lengths of up to 28 C atoms (Guschina and Harwood 2006). The presence of long-chain PUFAs is also reflected by the fatty acid composition of the thylakoid membrane lipids. In centric diatoms (*Skeletonema marinoi*, *Thalassiosira weissflogii*) and the pennate *P. tricornutum* MGDG contains the main long-chain PUFA of diatoms, i.e. eicosapentaenoic acid (EPA, 20:5) (Yongmanitchai and Ward 1993; Yan et al. 2011; Dodson et al. 2013; Dodson et al. 2014; Abida et al. 2015). EPA is preferentially bound to the sn-1 position of the glycerol backbone whereas C16 fatty acids with different amounts of double bonds (16:1, 16:2, 16:3, 16:4) can be observed at the sn-2 position. MGDG with C20:5 and C16:3 fatty acids seems to represent the majority of MGDG molecules in diatom thylakoids. Interestingly, EPA at the sn-1 position of the MGDG molecule can be replaced by other C20 fatty acids with a lower amount of double bonds like eicosatrienoic acid (20:3) or eicosatetraenoic acid (20:4). In addition to MGDG molecules with C20/C16 fatty acids, the recent analyses have presented evidence for the presence of MGDG molecules with C16 fatty acids at both the sn-1 and sn-2 position. Longer-chain PUFAs, like docosahexaenoic acid (DHA, 22:6), or C18 fatty acids are usually not found or detected in only minor concentrations in MGDG of centric diatoms and *P. tricornutum*.

The analyses by Yongmanitchai and Ward (1993), Yan et al. (2011), Dodson et al. (2013), Dodson et al. (2014) & Abida et al. (2015) also pointed out that the fatty acid composition of the main galactolipids MGDG and DGDG is comparable. EPA is the main fatty acid species at the sn-1 position of the DGDG molecule. The sn-2 position of DGDG is usually occupied by C16 fatty acids, and DGDG forms with C16 fatty acids at both the sn-1 and sn-2 positions can be observed. Like MGDG, DGDG molecules with the two fatty acids EPA (C20:5) and hexadecatrienoic acid (C16:3) seem to represent the majority of DGDG molecules in the diatom thylakoid membrane. Other pennate diatoms (*Haslea ostrearia* and *Navicula perminuta*) seem to exhibit a different fatty acid composition of the MGDG and DGDG molecules compared with the centric diatoms and *P. tricornutum* (Dodson et al. 2013). In these species, an enrichment of EPA cannot be detected and C18/C16 and C18/C18 forms of MGDG and DGDG are typically observed. The major forms of MGDG and DGDG seem to contain linolenic acid (18:3) and hexadecatrienoic acid (16:3) at the sn-1 and sn-2 positions, respectively. The fatty

acid composition of these pennate diatoms thus is comparable to the fatty acid composition of MGDG and DGDG of higher plants and green algae (Browse et al. 1986; Cho and Thompson 1987). However, this different lipid profile may be related to acclimation to environmental temperatures. Indeed, Dodson et al. (2014) could detect significant amounts of EPA in *H. ostrearia* at the sn-1 position of the MGDG and DGDG molecules under normal temperature conditions, whereas at high temperatures (30 °C) no EPA or other C20 fatty acids, but high concentrations of C18 fatty acids could be observed at the sn-1 position of MGDG and DGDG both in *H. ostrearia* and also *P. tricornutum*.

With regard to the anionic membrane lipids of diatoms, the fatty acid composition of SQDG of *P. tricornutum* (Yongmanitchai and Ward 1993; Abida et al. 2015) and that of SQDG and PG of three *Skeletonema* species has been analyzed (Yan et al. 2011). In contrast to MGDG and DGDG, the main part of SQDG present in diatom thylakoid membranes is enriched in fatty acids with a shorter chain length and C14 and C16 fatty acids are usually observed in both the sn-1 and sn-2 positions. The C14 and C16 fatty acids include C14:0, C16:0, C16:1 and C16:3 species. PG in *Skeletonema*, on the other hand, contains C18:1 fatty acids as the main molecular species.

1.3 Function of thylakoid membrane lipids

Thylakoid membrane lipids exert their functions on different structural levels. First, they build up the membrane bilayer in which the photosynthetic pigment protein complexes and the components of the electron transport chain are incorporated. Changes in the lipid and/or fatty acid composition of the thylakoid membrane as a reaction to changes in the environmental conditions, like e.g. temperature or light fluctuations, keep the membrane in a fluid state and thus maintain efficient electron transport and other membrane related processes such as the operation of the diadinoxanthin cycle (see below). The importance of a fluid state for the operation of biological membranes has first been described by Singer and Nicolson (1972). Recently, advances in our understanding of the fluid mosaic model with a special focus of different lipid phases in thylakoid membranes have been presented by Wilhelm et al. (2020).

With respect to the environmental factor light, Mock and Kroon (2002) observed an increase of the non-bilayer lipid MGDG accompanied by higher concentrations of EPA in sea ice diatoms which were grown under low light illumination. They proposed that the high contents of EPA were responsible for membrane fluidity and the velocity of the photosynthetic electron transport. Rousch et al. (2003) observed that the thermo-tolerant diatom *Chaetoceros muelleri* reacted with stronger changes in the fatty acid profile to temperature changes than the thermo-

intolerant *P. tricornutum*. Recently, Bojko et al. (2017) could show that the centric diatom *Thalassiosira pseudonana* reacted with an increase of PUFAs to a decrease of the cultivation temperature. The higher content of PUFAs resulted in a stabilization of the membrane fluidity and the PSII quantum yield at low temperatures. In addition to their role as membrane building blocks, thylakoid lipids serve as structural elements of the pigment proteins and play a role in the oligomerization of photosystems and light-harvesting complexes. Through an enrichment at the monomer-monomer interface MGDG seems to play a role in the establishment and maintenance of PSII dimers which represent the native state of PSII in the thylakoid membrane (Kern and Guskov 2011; Nagao et al. 2019a). PG is most likely involved in the trimerization of the PSII light-harvesting complex of higher plants, the LHCII, whereas DGDG is important for the structural integrity of the complex (Kühlbrandt et al. 1994).

Recently, the first molecular structure of a diatom pigment protein complex determined by x-ray crystallography has been published, namely that of the dimeric fucoxanthin chlorophyll binding protein (FCP) complex of *P. tricornutum* (Wang et al. 2019) (see "2.5 *Molecular structure of FCPs"*). Within the dimeric FCP two lipid molecules have been resolved, a PG and a DGDG molecule. Although the PG and DGDG molecules have not been assigned specific roles in the dimerization of the FCP, it was proposed that the two lipid molecules serve to stabilize the FCP dimers. The determination of the structure of a PSII-FCP supercomplex from the pennate diatom *Ch. gracilis* by cryo-electron microscopy revealed the presence of more than 100 lipid molecules in the PSII-FCP dimer (Pi et al. 2019; Wang et al. 2020). The majority of the lipids, comprising 20 DGDG, 42 MGDG, 16 SQDG and 30 PG molecules, are located at the interfaces of the PSII protein subunits which, according to Wang et al. (2020), argues for an important role in the establishment and stabilization of protein subunit interactions. A stabilizing role of thylakoid membrane lipids for the native structure of FCP complexes has also been reported in another study (Schaller-Laudel et al. 2017). In these experiments, the neutral galactolipids MGDG and DGDG exhibited the highest capacity for the stabilization of FCP complexes. For higher plants and cyanobacteria it has been shown that MGDG plays a role in targeting Q_B to its binding site at the stromal side of the PSII reaction center and that DGDG is important for the stabilization of the Oxygen Evolving Complex at the lumenal side of PSII (Kern and Guskov 2011). Although the first results concerning the structure of the diatom PSII core complex have been published (Wang et al. 2020), a detailed assignment of the lipid molecules within the core complex to specific functions is still missing. However, the structural and functional similarities between the diatom and higher plant and cyanobacterial PSII and PSI core complexes suggest a similar role of the thylakoid lipids in photosystems of diatoms.

Besides the lipids that build up the main lipid phase of the thylakoid membrane and those that serve as structural lipids embedded into the protein matrix, a third class of membrane lipids exist. These lipids are closely associated with the pigment protein complexes and form a lipid shield surrounding the complexes. In the LHCII of higher plants (Schaller et al. 2010) and the FCP complexes of the diatoms *P. tricornutum* and *C. meneghiniana* (Lepetit et al. 2010) the lipid shields are highly enriched in MGDG. MGDG serves to solubilize the hydrophobic xanthophyll cycle (XC) pigments violaxanthin, antheraxanthin and zeaxanthin in higher plants and diadinoxanthin (Dd) and diatoxanthin (Dt) in diatoms, thereby making these pigments accessible to the enzymes violaxanthin or diadinoxanthin de-epoxidase (Goss et al. 2005; Goss et al. 2007). *(Side note: The diadinoxanthin de-epoxidase is usually annotated as a violaxanthin de-epoxidase in diatom genomes. This reflects the fact that this enzyme can also de-epoxidize violaxanthin, which is a precursor in synthesis of the main diatom carotenoids fucoxanthin and Dd (Lohr and Wilhelm 1999).)* The XC has a dominant role in photoprotection of plants and diatoms (see "*Photosynthetic light reactions in diatoms. II. The dynamic regulation of the various light reactions*"). It has also been proposed that the local enrichment of MGDG leads to the establishment of a special lipid phase, the so-called inverted hexagonal (H_{II}) phase. This non-bilayer phase seems to be essential for the efficient conversion of XC pigments (Latowski et al. 2002; Latowski et al. 2004; Goss et al. 2005; Goss et al. 2007). The H_{II} phase together with the LHCII/FCP, the de-epoxidases and the XC pigments can be described as a special thylakoid membrane domain with a specific lipid and protein composition and a specific function, namely the enzymatic de-epoxidation of the XC pigments (Goss et al. 2017).

The XC pigments also influence the properties of the lipid phase of the membrane. The conversion of Dd to Dt leads to a stable increase of the rigidity of the hydrophobic core of the diatom thylakoid membrane and a dynamic stabilization of the peripheral membrane parts which can be observed during the ongoing de-epoxidation reaction (Bojko et al. 2019). The stabilization of diatom thylakoids by XC pigments has been suggested to play a role in the adaptation of the membrane to rapid changes in temperature.

1.4 Localization of thylakoid membrane lipids

Based on the findings that SQDG strongly inhibits the de-epoxidation of Dd to Dt (Goss et al. 2009) and that MGDG forms a lipid shield around the FCP complexes, which incorporates a large part of the XC pigments (Lepetit et al. 2010), a model for the lipid and protein distribution in the thylakoid membranes of diatoms was proposed (Lepetit et al. 2012). The model predicts

that the inner membranes of the typical stacks of three thylakoids are enriched in PSII and its associated FCP complexes (Fig. 1). The lipid composition of the inner membranes is dominated by MGDG and represents the place where efficient operation of the XC is taking place. SQDG, on the other hand, is enriched in the outer membranes of the thylakoid stacks so as not to interfere with the diadinoxanthin de-epoxidase. Outer membranes and margin regions of the stacks contain mainly PSI and the ATP synthase which thus gains access to the chloroplast stroma. Although the model was mainly based on physiological and biochemical data, recent structural data have confirmed several important aspects and predictions (Flori et al. 2017) (see also *"Introduction"*). Revealing also connections between the different thylakoid lamellae, the authors concluded that the three-dimensional network of the thylakoid membrane of diatoms is far more complex than the simple layout of three loosely connected membranes.

2. Light harvesting

Diatoms, like vascular plants, harvest light using membrane intrinsic proteins that belong to the light-harvesting complex (Lhc) protein family. Lhcs are characterized by three membrane spanning α-helices, whereby helix 1 and 3 form a cross-like superhelical structure. These proteins non-covalently attach chlorophylls (Chl) as well as carotenoids. Lhcs are connected with the photosystem core complexes, forming so-called photosystem supercomplexes. Major differences compared to plants can be found in the number of Lhcs associated with the photosystems, their specific structure, and the number and identity of pigments bound to the diatom light harvesting apparatus. In recent years there have been major advances in understanding the light harvesting machinery of diatoms which we will review here.

2.1 The diatom light harvesting systems

In diatoms Lhcs, Chl *a* and Chl c_1 (and little Chl c_2) (Fawley 1989; Kraay et al. 1992) are accompanied by the major carotenoid fucoxanthin (Fx), and usually by minor amounts of Dd and Dt. The diatom genome encodes large numbers of *Lhc* genes whose translated proteins fall into three major and some minor groups. The major groups include i) the main group of proteins working in light harvesting, named Lhcf, ii) Lhcs most closely related to those of red algae called Lhcr, and iii) the photoprotective proteins called LI818 or Lhcx, related to green algal LhcSR (Eppard and Rhiel 1998; Bailleul et al. 2010; Ghazaryan et al. 2016). The minor groups comprise iv) a small group of genes called *Lhcz*, v) the so called *RedCaps* (Engelken et al. 2012), and vi) some other sequences that do not belong to either group. *Lhcf* and *Lhcr* genes constitute the biggest groups with 8-17 and 9-14 members, respectively, when comparing the three best studied diatoms *P. tricornutum* (Bowler et al. 2008), *T. pseudonana* (Armbrust et al. 2004), and *Cyclotella meneghiniana* (Gundermann et al. 2019). Concerning *Lhcx*, numbers are smaller with 4-6 genes. However, numbers are even higher for e.g. *Fragilariopsis cylindrus* (Mock et al. 2017). For *P. tricornutum* as well as for *T. pseudonana*, expression of all those genes was proven either on mRNA or on protein level in cells and pigment-protein complexes (Nymark et al. 2009; Lepetit et al. 2010; Grouneva et al. 2011; Schober et al. 2019; Kansy et al. 2020), and for *C. meneghiniana* all Lhcf and some Lhcx proteins were found in different light harvesting complexes (Gundermann et al. 2019). Most of the proteins encoded for by *Lhc* genes assemble into multi-subunit complexes that are then called fucoxanthin-chlorophyll-protein complexes (FCP). Note that single Lhc proteins of diatoms sometimes are also called

FCP mainly for historical reasons, since the Lhc nomenclature was only introduced when the first whole genome sequences became available.

2.2 Subunit compositions of light harvesting complexes

As in vascular plants, the photosystems of diatoms are surrounded by light harvesting complexes, whereby some are more tightly bound to either PSII or PSI, forming PSII-FCP or PSI-FCP supercore complexes/supercomplexes, respectively. Besides, there is an additional pool of more loosely bound FCPs, which will be considered first. Early on pools of FCPs were isolated and characterized from the pennate diatom *P. tricornutum* (Alberte et al. 1981; Friedman and Alberte 1984; Gugliemelli 1984; Fawley and Grossman 1986; Owens and World 1986; Caron and Brown 1987; Owens 1988; Berkaloff et al. 1990; Lavaud et al. 2003; Guglielmi et al. 2005). Later, centric diatoms like *C. meneghiniana* or *T. pseudonana* were studied as well, and sub-populations of FCP complexes were differentiated. In the pennate *P. tricornutum*, only trimeric FCP complexes were found (Joshi-Deo et al. 2010; Grouneva et al. 2011) that, nonetheless, could interact to form yet larger complexes (Lepetit et al. 2007; Gardian et al. 2014). Further separation demonstrated the presence of three major trimers, with Lhcf5, Lhcf10 and Lhcf2, or Lhcf4 as main subunits, respectively, together with different other Lhcf polypeptides (Gundermann et al. 2013). Later, homodimers of Lhcf4 were found in crystals used for X-ray crystallography (Wang et al. 2019, see below). No members of the other Lhc families (Lhcr or Lhcx) were found in purified trimeric FCPs of pennates so far (Gundermann et al. 2013), although the photoprotective Lhcx as well as Lhcr proteins are present when isolating the whole pool of FCP complexes (Lepetit et al. 2010; Nagao et al. 2013a; Taddei et al. 2018). In contrast, trimeric and specific higher oligomeric complexes were isolated from *C. meneghiniana*, a centric diatom (Büchel 2003), and two different complexes were later verified for other centrics as well, *T. pseudonana* (Grouneva et al. 2011) and *Ch. gracilis* (Nagao et al. 2012; Nagao et al. 2013a), respectively. In the centrics *C. meneghiniana* and *T. pseudonana*, Lhcf proteins accompanied by Lhcx1 proteins defined the major trimeric complex, named FCPa. The oligomeric complex with distinct Lhcf composition, named FCPb, was proven to be a nonamer (Röding et al. 2018). In *Ch. gracilis*, the oligomeric complex was named FCP-A and the trimeric complex FCP-B/C due to their subunit composition (Nagao et al. 2012; Nagao et al. 2013a). Recently, FCPa and FCPb complexes of *C. meneghiniana* were further divided into sub-complexes (Gundermann et al. 2019). Four different trimeric FCPa complexes were shown to exist, whereby FCPa3 and FCPa4 were the most abundant forms. Lhcf1 was the major polypeptide in both, accompanied by Lhcx1 in case of FCPa4. For FCPb two sub-complexes

were distinguished: FCPb1 that is built almost solely of Lhcf3, and FCPb2 that in addition contains Lhcx1 and Lhcx6_1 when isolated from cells grown under high light. When using sucrose gradient centrifugation to separate solubilized thylakoid membrane proteins, two bands were obtained, whereby the upper band contained associations of FCPa4, FCPa1 and FCPb2, i.e. those complexes that contain Lhcx1, whereas the lower band was an association of the remaining FCPa trimers and FCPb nonamers devoid of Lhcx1.

Lhcx1 is very similar in sequence in centrics and pennates, but only in centrics it was found in FCP trimers so far. It was proven to be involved in photoprotection in whole cells in both groups (Bailleul et al. 2010; Zhu and Green 2010; Ghazaryan et al. 2016; Buck et al. 2019) (see *Photosynthetic light reactions in diatoms. II. The dynamic regulation of the various light reactions"*). For *C. meneghiniana* it could also be shown that suppression of the fluorescence quenching of FCPa depends on Lhcx1 content, pH and aggregation (Gundermann and Büchel 2012), whereby Lhcx1 *in vivo* does not seem to act as direct quencher, but probably promotes FCPa aggregation (Ghazaryan et al. 2016), in line with the proposed uncoupling of the peripheral antennae upon induction of qE in pennates (Buck et al. 2019). Regarding the other Lhcx proteins, very little is known about their specific localization in the thylakoid membrane. For Lhcx3 of *P. tricornutum*, some evidence exists for a binding to the FCP complexes and to PSI, but further experiments are needed to corroborate this result (Taddei et al. 2018).

Only pennate diatoms like *P. tricornutum* have a 'red antenna' when cultivated under red light (Herbstová et al. 2015; Herbstová et al. 2017), characterized by a long wavelength fluorescence at around 710 nm at room temperature that is attributed to PSII. The main component of this red fluorescing antenna is Lhcf15, a protein which is not closely related to the other main Lhcf proteins that constitute the trimers and which has no close homologue in centrics. This red-shifted antenna was interpreted as an evolutionary adaptation towards survival in shaded environments. Recently, however, results demonstrated that the 'red antenna' may also be induced under weak green and yellow light (Oka et al. 2020).

2.3 FCPs associated with PSI

PSI-FCP supercores were isolated before sequences of Lhcs became known, and accordingly no detailed attribution of protein isoforms to complexes was initially possible (Berkaloff et al. 1990; Brakemann et al. 2006; Veith and Büchel 2007; Ikeda et al. 2008). Later, the homology of Lhcr with the red algal PSI antenna proteins gave rise to the assumption that Lhcr polypeptides fulfill the same function. Indeed, Lhcr proteins can be found in PSI isolates (Veith et al. 2009; Lepetit et al. 2010; Grouneva et al. 2011). Depending on the isolation procedure,

Lhcr are the sole PSI antennae components (Lepetit et al. 2010), or Lhcf (and sometimes Lhcx) proteins were present in the PSI antenna as well (Brakemann et al. 2006; Veith and Büchel 2007; Ikeda et al. 2008; Veith et al. 2009; Grouneva et al. 2011; Juhas and Büchel 2012; Ikeda et al. 2013; Calvaruso et al. 2020; Nagao et al. 2020). As in vascular plants, PSI of diatoms is a monomer (Veith and Büchel 2007; Ikeda et al. 2008; Nagao et al. 2020). In *Ch. gracilis*, the antenna complexes that serve PSI are characterized by long wavelength absorbing Chls that rapidly equilibrate with Chls in the PSI core through uphill energy excitation transfer (Nagao et al. 2018; Nagao et al. 2019b).

From the same organism the structure of a PSI-FCP supercomplex at 2.4 Å resolution became available recently (Nagao et al. 2020). Sixteen monomeric Lhcs surround the highly conserved core, i.e. much more Lhc subunits than in any other organism studied so far. Ten of those are Lhcr proteins and the others belong to a group that was named Lhcq and is closely related to Lhcf. The Lhc subunits are called Fcpa in the corresponding publication (Nagao et al. 2020), but the respective Lhcr/Lhcq names can be found in the protein data bank file (pdb file 6L4U). Nine Fcpa are surrounding the core in a circle that is almost closed (Fcpa1-9), whereby only the PsaL/I side is not binding any Lhc. These Lhc all belong to the Lhcr family. On the PsaA side, Fcpa10-16 are found in addition, whereby only Fcpa10 belongs to the Lhcr group, and the others are Lhcq proteins. Pigment binding differs strongly between the Fcpa subunits: five to thirteen Chl *a*, none to seven Chl *c*, one to seven Fx and one to four Dd are found. For example, the subunit called Fcpa15 has the highest pigment load with 13 Chl *a*:0 Chl *c*:7 Fx:2 Dd, whereas Fcpa1 carries only a small amount of pigments (6 Chl *a*:2 Chl *c*:2 Fx:1 Dd). Fcpa13 is very unusual with a high Chl c and low Fx content (6:6:2:1). More recently, the structure of an even bigger PSI-FCP complex from *Ch. gracilis* was solved (Xu et al. 2020). Here, 24 monomeric FCP surround the monomeric PSI cores. Unfortunately, neither protein nor pigment attribution are identical for the FCP complexes present in both structures.

2.4 FCPs associated with PSII

A lot of detail is also known about PSII-FCP supercores, since the structure of such a complex at high resolution from *Ch. gracilis* became also available recently (Nagao et al. 2019a; Pi et al. 2019). The core dimer of PSII is highly homologous to that of vascular plants and especially red algae, but the organization of the surrounding FCPs differs. Diatoms lack homologues to the minor antenna proteins CP24, CP26, and CP29 of plants, but nonetheless monomeric Lhc are found, albeit in totally different positions. Comparable to the situation in vascular plants, where light-harvesting complex II (LHCII) is found in the supercores, two strongly bound (S)

and two less tightly bound (M) oligomers of FCPs are present in the dimeric PSII supercores (Fig. 2A). However, these FCPs are tetrameric in *Ch. gracilis*, in contrast to the trimers or nonamers reported for the free pool of FCPs in the same species. Since *Ch. gracilis* is not sequenced, only some Lhc sequences could be used for model building. According to Pi et al. (2019), the tetramers consist of FCP-A, i.e. the polypeptide found in the nonamers of the free FCP pool before. Due to the lack of sequences, the homologous sequence from *T. pseudonana* (Lhcf8) was used for modelling. In contrast, Nagao et al. (2019a) attributed the subunits of the tetramer to Lhcf1, a constituent of the trimeric complexes in other centrics. However, since the resolution of the PSII-FCP supercore structures is at 3.0 and 3.6 Å, respectively, slight variations in the electron densities between monomers might suggest that the tetramers consist of several, very similar Lhc proteins. Concerning the monomeric subunits, one (FCP-D) turned out to be an antenna protein of the Lhcr group (Pi et al. 2019). The others could not be unambiguously identified. Very recently, a low resolution structure of the PSII-FCP complex of *T. pseudonana* was published (Arshad et al. 2021). The overall arrangement with three monomeric and two oligomeric FCP complexes resembled closely the structure of PSII from *Ch. gracilis*. However, the oligomeric FCPs appeared as trimers, not as tetramers, in accordance with the trimeric FCPs from the free FCP pool of *T. pseudonana*.

In summary, surprisingly, three different oligomeric states of FCPs exist besides monomeric Lhcs when considering pennate and centric diatoms together, whereas in plants only trimeric complexes (LHCII) and dimers (LHCI) are found. The recently available structures of a supercore from centrics (*Chaetoceros*) (Nagao et al. 2019a; Pi et al. 2019) and an FCP from pennates (*Phaeodactylum*) (Wang et al. 2019) were combined by Wang et al. (2020) into a model where the supercore having tetrameric FCPs bound is surrounded by a pool of dimeric FCPs. However, for the centrics *C. meneghiniana* as well as *T. pseudonana* trimeric FCPs were demonstrated by imaging methods to constitute the pool of peripheral FCPs and the PSII associated FCPs, respectively(Röding et al. 2018, Arshad et al. 2021). In addition, no data are available about the oligomeric state of the remaining FCPs in pennates (built of other subunits than Lhcf4), and no structure of the PSII supercomplex is available. Using biochemical analyses, trimers were found in both groups of diatoms. In addition, in centric diatoms nonamers of specific polypeptide composition are present (Beer et al. 2006; Grouneva et al. 2011; Nagao et al. 2013a). For PSI the situation is much more clear, since only monomeric Lhcs are attached (Veith and Büchel 2007; Nagao et al. 2019b; Nagao et al. 2020, Xu et al. 2020).

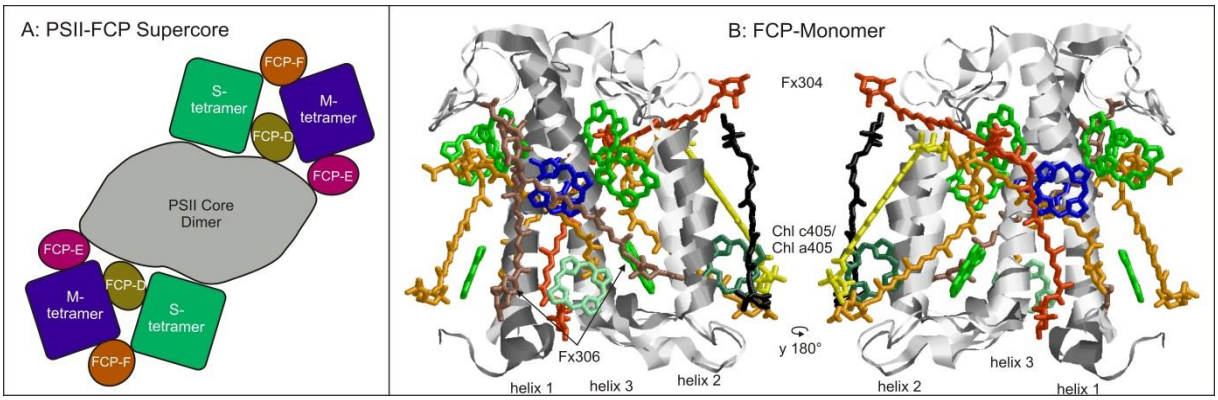

Figure 2

A: Scheme of the PSII-FCP supercore complex according to Nagao et al. (2019a) and Pi et al. (2019). The core of PSII, with the reaction center proteins D1 and D2 and the inner antenna proteins CP43 and CP47, is almost identical in plants and diatoms and shown in grey. PSII is a dimer, surrounded by FCP complexes on both sides. FCP-A, the subunit of both tetramers (ST and MT) was modelled using *T. pseudonana* Lhcf8 in case of Pi et al. (2019) and identified as Lhcf1 by Nagao et al. (2019a). Note that in *T. pseudonana* these complexes are trimeric (Arshad et al. 2021). FCP-D corresponds to Lhca2, a protein of the Lhcr group. FCP-E and FCP-F could not be identified.

B: Overlay of one of the monomers of the S-tetramer (taken from pdb 6JLU, 3.0 Å resolution, Pi et al. 2019) with one monomer of the dimeric FCP out of Lhcf4 of *P. tricornutum* (pdb 6A2W, 1.8 Å resolution, Wang et al. 2019). Since the structure of the M-tetramers as well as the tetramers by Nagao et al. (2019a) (pdb 6J40, 3.6 Å) closely resembles the shown structure, they are omitted from the comparison. The protein backbone is depicted in grey (6JLU) and white (6A2W), respectively. The pigments in (nearly) identical sites in both complexes are omitted for the dimeric FCP and shown in colors for the ST-FCP: Chl *a* in green and Chl *c* in blue, whereby Chl 405, which was attributed to Chl *a* in the dimeric FCP and to Chl *c* in the tetramers, is shown in blue-green. The Chl *a* not found in the dimeric FCP (and M-tetramers), but in S-tetramers is depicted in light-green. The four Fx molecules present in identical locations in the dimer and the tetramers are shown in orange, whereas the Fx molecule present only in the tetrameric FCPs is shown in yellow. Fx306 is oriented more perpendicular to the membrane plane in the FCP dimer, whereas it adopts a different orientation in some subunits of the tetramers; both orientations are given in brown color. The additional Fx molecules and the Dd only present in the dimer are shown in red and black, respectively. The left panel shows the same complexes as the right panel, but turned by 180° around the y-axis.

2.5 Molecular structure of FCPs

The first molecular structure at high resolution (1.8 Å) of a dimeric FCP of Lhcf4 from *P. tricornutum* became available recently (Wang et al. 2019), and the overall features were confirmed for the FCPs within the PSII-FCP and PSI-FCP supercomplexes (Nagao et al. 2019a;

Pi et al. 2019; Nagao et al. 2020) (Fig. 2B). The overall protein scaffold structure of FCP monomers is similar to that of LHCII monomers (for an overview see Büchel 2019). The helices where sequence conservation is high, i.e. helix 1 and 3, adopt an almost identical configuration in FCP vs. LHCII, whereas helix 2 has a slightly different location and tilt that also differs between the FCP-dimer from *P. tricornutum* and the FCP-tetramers from *Ch. gracilis* found in PSII-supercomplexes. The complex from *P. tricornutum* was crystallized as a dimer, whereby the connection between the monomers was due to strong interactions between helices 2. This 'head to head' configuration has not been shown before for any member of the Lhc family, since e.g. Lhca1/Lhc4 dimers of plant PSI interact in a 'head to tail' configuration (Ben-Shem et al. 2003). Similarly, the monomers of the M- and S-tetramer in the PSII-FCP supercore complexes are associated 'head to tail'. In contrast to LHCII, where helices 3 come close to the stromal surface, the subunits of the tetramers are turned by 180° in comparison to LHCII, so that helices 1 approach closest to the stromal side (Nagao et al. 2019a; Pi et al. 2019). Although helices 1 and 3 are almost identical in FCP and LHCII, the dimer and the tetramers are arranged in a way that these helices adopt a slightly different tilt with respect to the membrane plane compared to the arrangement in the trimeric LHCII (Liu et al. 2004; Standfuss et al. 2005; Büchel 2019).

Seven Fx, one Dd, seven Chl *a*, and two Chl *c* per monomer were fitted into the electron density map of the *P. tricornutum* FCP-dimer (Wang et al. 2019), whereas in the tetrameric FCPs of *Ch. gracile* only six Fx, but nine (M-tetramer) or ten Chl molecules (S-tetramer) were found (Pi et al. 2019; Wang et al. 2019) (Fig. 2B), and, as stated above, the variability is even larger in PSI associated Lhc. In general, the Chl:carotenoid ratio is much lower than in plant LHCII. As already anticipated from sequence comparisons and based on spectroscopy data (Premvardhan et al. 2010), six of the Chl binding sites are highly conserved between LHCII and FCP, with the central Fx molecules arranged close to helix 1 and 3 similarly to the luteins in LHCII (Liu et al. 2004; Standfuss et al. 2005). One Dd was fitted in a more peripherally located density in the *P. tricornutum* FCP-dimer, but was not found in any of the *Ch. gracilis* tetramers (Fig. 2B). The porphyrin rings of Chl *c* and Chl *a* are rather similar in structure, so Chl *c* can only be distinguished from Chl *a* due to the planarity of the C18=C17 double bonds and the lack of phytol in Chl *c*, which requires a high resolution electron density map to resolve. In the diatom FCP-tetramers close to PSII, three Chl *c* were assigned, the additional one being Chl *c*405 (nomenclature according to Wang et al. 2019), a binding site that had been assigned to Chl *a* in the FCP-dimer of *P. tricornutum* only for reasons of pigment stoichiometry (Wang et al. 2019). Surprisingly, Chl *c*403 and Chl *c*408 reside in the strongly conserved binding sites

603 (Chl *c*403) and 612 (Chl *c*408), occupied by Chl *a* in case of LHCII. Both Chl *c*'s are in close contact with Fx molecules, which are bound in places where no carotenoids are found in case of LHCII. All carotenoid molecules in FCP are in *all-trans* configuration, and all have Chl *a* molecules in close vicinity (3.1 to 3.6 Å). Whereas the Chl binding sites are highly conserved between the FCP-dimer and the FCP-tetramer structures, only four Fx are found in identical places to LHC carotenoids (Fig. 2B), including those in the lutein binding sites. The Fx interacting with one of the Chl *c* in the Chl *a*/Chl *c*/Chl *a* clusters (Fx306) is oriented almost perpendicular to the membrane plane in the FCP-dimers and in some subunits of the tetramers, whereas it is oriented in an angle of almost 45° in others. Two Fx are found in totally different locations in tetramers compared to the dimer. The most peculiar Fx is Fx304 in the FCP-dimer, running almost parallel to the membrane plane on the stromal side. This Fx is missing in the FCP-tetramers.

2.6 Excitation energy transfer in FCPs

Pigment ratios of around 6-8 Chl *a* : 2-3 Chl *c* : 6-8 Fx were reported for the different diatom FCP complexes (which represented rather the main, free pool of FCP complexes), depending on growth condition, isolation procedure and species (Papagiannakis et al. 2005; Beer et al. 2006; Lepetit et al. 2007; Joshi-Deo et al. 2010; Lepetit et al. 2010; Gundermann and Büchel 2012; Nagao et al. 2013b). More evident differences were reported concerning the PSI associated Lhc antennae proteins: For both centric and pennate diatoms the Chl *c*/Fx ratio was lower, whereas the (Dd+Dt)/Fx ratio was strongly increased (Lepetit et al. 2007; Veith and Büchel 2007; Veith et al. 2009; Lepetit et al. 2010; Juhas and Büchel 2012). The Chl *c*/Fx ratio was even lower when *P. tricornutum* was grown under red light (Bína et al. 2016). Whereas this pigmentation is obviously due to the presence of the different Lhcf and Lhcr polypeptides, respectively, nothing is known so far about the pigmentation of the gene products of *RedCaps*, *Lhcy* or *Lhcz* that have been solely analyzed on genetic level so far. Even for Lhcx proteins the question of whether they are pigmented remains open, since they have not been isolated as single proteins so far. However, their high similarity to the pigmented LhcSR proteins of green algae (Bonente et al. 2011) is a strong argument for diatom Lhcx proteins binding pigments (see *"Photosynthetic light reactions in diatoms. II. The dynamic regulation of the various light reactions"*).

In FCPa and FCPb complexes of *C. meneghiniana*, two differently bound Chl *c* molecules were identified by Resonance Raman spectroscopy (Premvardhan et al. 2010) and also in 2D spectroscopy by their different transfer times (Songaila et al. 2013; Gelzinis et al. 2015), in

agreement with the numbers although not the locations found in the crystal structure for *P. tricornutum* Lhcf4 (Wang et al. 2019). In all FCPs isolated so far, the Q_Y absorption of FCPs is at relatively short wavelength (~671 nm), excluding close excitonic interactions between Chl *a* molecules as verified by CD spectra, where no excitonic interactions are visible in the Q_Y (Büchel 2003; Szábo et al. 2008; Joshi-Deo et al. 2010). The fact that the strong Chl *a* interaction of a610/a611/a612 visible in LHCII (Novoderezhkin et al. 2004) is broken by Chl *c* in FCPs, also due to slightly different arrangement of Chl *a*401 (FCP) compared to Chl *a*611 (LHCII), is also in line with the lack of excitonic interactions. Thus, delocalized excited states are missing, which contribute to the robustness of energy transfer in the flexible protein environment e.g. in LHCII of vascular plants. FCP complexes, in contrast, seem to use subtle changes in protein scaffold conformation to switch frequently into low-energy states with improved light-harvesting properties as shown for FCPa from *C. meneghiniana* (Krüger et al. 2017).

Fx is actively involved in energy transfer to Chl *a*. Fx is special since it has a carbonyl moiety in conjugation with the polyene backbone. Carotenoids are in principle able to transfer energy from both their lowest singlet excited states, i.e. S_1 and S_2, but direct absorption into S_1 is forbidden due to their symmetry. In Fx an additional excited state with an intramolecular charge transfer (ICT) character exists. This ICT state can be coupled to the S_1 state, and plays a major role in carotenoid-Chl energy transfer (Bautista et al. 1999; Vaswani et al. 2003; Zigmantas et al. 2004; Papagiannakis et al. 2005; Premvardhan et al. 2005; Gelzinis et al. 2015; West et al. 2018). In addition, Fx displays an extreme bathochromic shift upon protein binding, extending the absorption from 390 nm up to 580 nm. More 'blue', 'green' and 'red' absorbing Fx molecules were detected in FCPa as well as in FCPb from *C. meneghiniana* (Premvardhan et al. 2008; Premvardhan et al. 2009; Premvardhan et al. 2010) using Stark and Resonance Raman spectroscopy, but could so far not be attributed to certain Fx molecules in the structure. 'Blue' and 'red' Fx were also demonstrated for whole cells of *C. meneghiniana* and *P. tricornutum* using electrochromic shift measurements (Szábo et al. 2010). Excitation energy transfer from Fx to Chl *a* proceeds mainly via the S_1/S_{ICT} state in FCPs, whereby the transfer to the Q_Y state of Chl *a* has a time constant of 0.6 ps in FCPa of *C. meneghiniana* (Papagiannakis et al. 2005; Gildenhoff et al. 2010a). The transfer for the Fx S_2 state directly into the Q_X state of Chl *a* is even faster with <150 fs (Gildenhoff et al. 2010a). For *P. tricornutum*, two routes using the S_1/S_{ICT} state were determined recently, whereby the slower (~ 6 ps) route uses the S_1 part of the potential surface of the S_1/S_{ICT} equilibrium (West et al. 2018). The fast Fx to Chl *a* transfer is

possible due to the arrangement of Fx and Chl *a*: each Fx has an Chl *a* molecule in close vicinity as stated above. Fx also acts as an efficient quencher of Chl *a* triplets (Di Valentin et al. 2012). Fx-Fx transfer with a time constant of 25 ps was measured using FCPa of *C. meneghiniana* (Gildenhoff et al. 2010a; Gildenhoff et al. 2010b). However, no pair of Fx molecules can be pinpointed in the structures responsible for this route of excitation energy transfer.

No energy transfer from Fx to Chl *c* was observed within the limit of instrumentation of pump-probe as well as 2D spectroscopy for *C. meneghiniana* FCPs (Papagiannakis et al. 2005; Gildenhoff et al. 2010a; Songaila et al. 2013; Gelzinis et al. 2015). 2D spectroscopy also revealed that the two Chl *c* have different time constants for energy transfer into Chl *a*, both reactions being extremely fast with 60 fs and less, respectively (Songaila et al. 2013; Gelzinis et al. 2015). This is in agreement with the close contact of Chl *c* and Chl *a*, allowing fast excitation energy transfer between these pigments. Judging from the structure, also the Fx/Chl *c* arrangement is, however, perfectly suited for fast excitation energy transfer. If present, it has to be even faster than Chl *c*-Chl *a* transfer in order to have escaped detection.

The differences might be due to the fact that spectroscopically mainly the trimeric FCPs from *C. meneghiniana* were analyzed, whereas structural data come from the dimeric FCP of *P. tricornutum*. The contradictions between the structure and the wealth of spectroscopic data were recently highlighted (Gelzinis et al. 2020). More structures are evidently needed in order to fully understand excitation energy transfer in FCP.

In the PSII-FCP supercore complex, energy pathways have only been deduced from the structure so far. The distances between Chls imply that the S-tetramers funnel energy into CP47, one of the inner antenna proteins of PSII, via a Chl *a* binding subunit called PsbG that is not present in vascular plant PSII, and into FCP-D (Fig. 2A). From the latter the energy can be transferred to CP43, the inner antenna on the opposite side of the PSII reaction center compared to CP47. The M-tetramer might transfer energy via FCP-E and FCP-D also into the Chls bound to CP43. FCP-F is rather peripheral and thus probably delivers energy mainly to the M-tetramer. Also for the PSI-FCP complexes an excitation energy transfer network was proposed, with pathways in between the inner ring of Lhc proteins as well as pathways from the more peripheral antenna into the inner ring and from there to the core. Since the methods to prepare supercore complexes in sufficient amounts for ultrafast spectroscopy are available now, these pathways will probably be elucidated in more detail in future.

Outlook

The recently obtained structures of PSII and PSI supercomplexes allow for the first time detailed insights into particular steric features of the whole light harvesting system and the excitation energy routes in diatoms. We need more of these structures, obtained from diatoms in different acclimation states but also from different species. This way, we may reveal the localization of the Lhcx proteins as well of those proteins which so far have only been found on the genetic level, such as *Lhcz* or *Redcap*. More of these studies will also enable us to resolve some so far existing discrepancies about the composition and oligomerisation states of FCPs obtained either by classical biochemical preparations or by crystallization approaches. In addition, the dynamic interaction between thylakoid lipid domains and thylakoidal protein complexes in diatoms is a field which is as yet largely understudied and would also profit from sophisticated imaging approaches. In this regard, we also need to better understand biogenesis of thylakoid membranes and photosynthetic complexes. Recently, first insights regarding the insertion of FCPs in *P. tricornutum* have been obtained. Alb3b, a protein functioning in the insertion and assembly of thylakoid membrane protein complexes in plants, was demonstrated to be essential for FCP assembly (Nymark et al. 2019). On the other hand, the chloroplast signal recognition particle protein CpSRP54, involved in targeting LHC to the chloroplast membrane in plants and green algae, is not involved in FCP accumulation but important for the insertion of plastid encoded thylakoid membrane proteins (Nymark et al 2021). This paves the way for future studies on FCP assembly, but to fully understand this process, also the enzymes working in Fx and Chl *c* synthesis still need to be identified.

References

Abida H, Dolch L-J, Meï C, Villanova V, Conte M, Block MA, . . . Maréchal E (2015) Membrane glycerolipid remodeling triggered by nitrogen and phosphorus starvation in *Phaeodactylum tricornutum*. Plant Physiol 167 (1):118-136.

Alberte RS, Friedman AL, Gustafson DL, Rudnick MS, Lyman H (1981) Light harvesting systems of brown algae and diatoms. Isolation and characterization of chlorophyll a/c and chlorophyll a/fucoxanthin pigment protein complexes. Biochimica et Biophysica Acta 635:304-316.

Anderson JM (1999) Insights into the consequences of grana stacking of thylakoid membranes in vascular plants: a personal perspective. Funct Plant Biol 26 (7):625-639.

Arshad R, Calvaruso C, Boekema EJ, Büchel C, Kouřil R (2021) Revealing the architecture of the photosynthetic apparatus in the diatom *Thalassiosira pseudonana*. Plant Physiol 186 (4):2124-2136.

Bailleul B, Rogato A, de Martino A, Coesel S, Cardol P, Bowler C, . . . Finazzi G (2010) An atypical member of the light-harvesting complex stress-related protein family modulates diatom responses to light. Proc Natl Acad Sci USA 107 (42):18214-18219.

Bautista JA, Connors RE, Raju BB, Hiller RG, Sharples FP, Gosztola D, . . . Frank HA (1999) Excited state properties of peridinin: observation of a solvent dependence of the lowest excited singlet state lifetime and spectral behavior unique among carotenoids. J Phys Chem B 103 (41):8751-8758.

Beer A, Gundermann K, Beckmann J, Büchel C (2006) Subunit composition and pigmentation of fucoxanthin-chlorophyll proteins in diatoms: Evidence for a subunit involved in diadinoxanthin and diatoxanthin binding. Biochemistry 45 (43):13046-13053.

Ben-Shem A, Frolow F, Nelson N (2003) Crystal structure of plant photosystem I. Nature 426 (6967):630-635.

Berkaloff C, Caron L, Rousseau B (1990) Subunit organization of PSI particles from brown algae and diatoms: polypeptide and pigment analysis. Photosynth Res 23:181-193.

Biggins J, Bruce D (1989) Regulation of excitation energy transfer in organisms containing phycobilins. Photosynth Res 20 (1):1-34.

Bína D, Herbstová M, Gardian Z, Vácha F, Litvín R (2016) Novel structural aspect of the diatom thylakoid membrane: lateral segregation of photosystem I under red-enhanced illumination. Sci Rep 6:25583.

Bojko M, Olchawa-Pajor M, Chyc M, Goss R, Schaller-Laudel S, Latowski D Acclimatization of *Thalassiosira pseudonana* photosynthetic membranes to environmental temperature changes. In: Proceedings of the 3rdWorld Congress on New Technologies, 2017. doi:DOI: 10.11159/icepr17.120

Bojko M, Olchawa-Pajor M, Goss R, Schaller-Laudel S, Strzałka K, Latowski D (2019) Diadinoxanthin de-epoxidation as important factor in the short-term stabilization of diatom photosynthetic membranes exposed to different temperatures. Plant Cell Environ 42:1270-1286.

Bonente G, Ballottari M, Truong TB, Morosinotto T, Ahn TK, Fleming GR, . . . Bassi R (2011) Analysis of Lhcsr3, a protein essential for feedback de-excitation in the green alga *Chlamydomonas reinhardtii*. PLoS Biol 9 (1):e1000577.

Brakemann T, Schlormann W, Marquardt J, Nolte M, Rhiel E (2006) Association of fucoxanthin chlorophyll a/c-binding polypeptides with photosystems and phosphorylation in the centric diatom *Cyclotella cryptica*. Protist 157 (4):463-475.

Browse J, Warwick N, Somerville CR, Slack CR (1986) Fluxes through the prokaryotic and eukaryotic pathways of lipid synthesis in the '16:3' plant *Arabidopsis thaliana*. Biochem J 235 (1):25-31.

Büchel C (2003) Fucoxanthin-chlorophyll proteins in diatoms: 18 and 19 kDa subunits assemble into different oligomeric states. Biochemistry 42:13027-13034.

Büchel C (2015) Evolution and function of light harvesting proteins. J Plant Physiol 172:62-75.

Büchel C (2020) Light harvesting complexes in chlorophyll c-containing algae. BBA-Bioenergetics 1861:148027.

748 Buck JM, Sherman J, Bártulos CR, Serif M, Halder M, Henkel J, . . . Lepetit B (2019) Lhcx proteins provide
749 photoprotection via thermal dissipation of absorbed light in the diatom *Phaeodactylum*
750 *tricornutum*. Nat Commun 10 (1):4167.
751 Calvaruso C, Rokka A, Aro E-M, Büchel C (2020) Specific Lhc proteins are bound to PSI or PSII
752 supercomplexes in the diatom *Thalassiosira pseudonana*. Plant Physiol
753 DOI:10.1104/pp.20.00042.
754 Canavate JP, Armada I, Rios JL, Hachero-Cruzado I (2016) Exploring occurrence and molecular diversity
755 of betaine lipids across taxonomy of marine microalgae. Phytochemistry 124:68-78.
756 Caron L, Brown J (1987) Chlorophyll-carotinoid protein complexes from the diatom *Phaeodactylum*
757 *tricornutum*:spectrophotometric, pigment and polypeptide analyses. Plant Cell Physiol 28:775-
758 785.
759 Cho SH, Thompson G (1987) On the metabolic relationships between monogalactosyldiacylglycerol and
760 digalactosyldiacylglycerol molecular species in *Dunaliella salina*. J Biol Chem 262 (16):7586-
761 7593.
762 Croce R, van Amerongen H (2020) Light harvesting in oxygenic photosynthesis: Structural biology
763 meets spectroscopy. Science 369 (6506):eaay2058.
764 Di Valentin M, Buchel C, Giacometti GM, Carbonera D (2012) Chlorophyll triplet quenching by
765 fucoxanthin in the fucoxanthin-chlorophyll protein from the diatom *Cyclotella meneghiniana*.
766 Biochem Biophys Res Commun 427 (3):637-641.
767 Dodson VJ, Dahmen JL, Mouget J-L, Leblond JD (2013) Mono- and digalactosyldiacylglycerol
768 composition of the marennine-producing diatom, *Haslea ostrearia*: Comparison to a selection
769 of pennate and centric diatoms. Phycol Res 61 (3):199-207.
770 Dodson VJ, Mouget J-L, Dahmen JL, Leblond JD (2014) The long and short of it: temperature-dependent
771 modifications of fatty acid chain length and unsaturation in the galactolipid profiles of the
772 diatoms *Haslea ostrearia* and *Phaeodactylum tricornutum*. Hydrobiologia 727 (1):95-107.
773 Dorrell RG, Gile G, Mccallum G, Méheust R, Bapteste EP, Klinger CM, . . . Bowler C (2017) Chimeric
774 origins of ochrophytes and haptophytes revealed through an ancient plastid proteome. Elife
775 6:e23717.
776 Engelken J, Funk C, Adamska I (2012) The extended light-harvesting complex (LHC) protein superfamily:
777 Classification and evolutionary dynamics. in R Burnap, W Vermaas, eds, Functional Genomics
778 and Evolution of Photosynthetic Systems, Volume 33, Springer:265-284.
779 Eppard M, Rhiel E (1998) The genes encoding light-harvesting subunits of *Cyclotella cryptica*
780 (Bacillariophyceae) constitute a complex and heterogeneous family. Mol Genet Genomics 260
781 (4):335-345.
782 Falkowski PG, Fenchel T, Delong EF (2008) The microbial engines that drive earth's biogeochemical
783 cycles. Science 320 (5879):1034-1039.
784 Fawley MW (1989) A new form of chlorophyll c involved in light-harvesting. Plant Physiol 91 (2):727-
785 732.
786 Fawley MW, Grossman AR (1986) Polypeptides of a light-harvesting complex of the diatom
787 *Phaeodactylum tricornutum* are synthesized in the cytoplasm of the cell as precursors. Plant
788 Physiol 81:149-155.
789 Flori S, Jouneau P-H, Bailleul B, Gallet B, Estrozi LF, Moriscot C, . . . Finazzi G (2017) Plastid thylakoid
790 architecture optimizes photosynthesis in diatoms. Nat Commun 8:15885.
791 Friedman AL, Alberte RS (1984) A diatom light-harvesting pigment-protein complex. Plant Physiol
792 76:483-489.
793 Gardian Z, Litvín R, Bína D, Vácha F (2014) Supramolecular organization of fucoxanthin–chlorophyll
794 proteins in centric and pennate diatoms. Photosynth Res 121 (1):79-86.
795 Gelzinis A, Augulis R, Büchel C, Robert B, Valkunas L (2021) Confronting FCP structure with ultrafast
796 spectroscopy data: evidence for structural variations. Phys Chem Chem Phys 23 (2):806-821.
797 Gelzinis A, Butkus V, Songaila E, Augulis R, Gall A, Büchel C, . . . Valkunas L (2015) Mapping energy
798 transfer channels in fucoxanthin–chlorophyll protein complex. BBA-Bioenergetics 1847
799 (2):241-247.

800 Ghazaryan A, Akhtar P, Garab G, Lambrev PH, Büchel C (2016) Involvement of the Lhcx protein Fcp6 of
801 the diatom *Cyclotella meneghiniana* in the macro-organisation and structural flexibility of
802 thylakoid membranes. BBA-Bioenergetics 1857 (9):1373-1379.
803 Gildenhoff N, Amarie S, Gundermann K, Beer A, Büchel C, Wachtveitl J (2010a) Oligomerization and
804 pigmentation dependent excitation energy transfer in fucoxanthin-chlorophyll proteins. BBA-
805 Bioenergetics 1797 (5):543-549.
806 Gildenhoff N, Herz J, Gundermann K, Büchel C, Wachtveitl J (2010b) The excitation energy transfer in
807 the trimeric fucoxanthin–chlorophyll protein from *Cyclotella meneghiniana* analyzed by
808 polarized transient absorption spectroscopy. Chem Phys 373 (1-2):104-109.
809 Goss R, Greifenhagen A, Bergner J, Volke D, Hoffmann R, Wilhelm C, Schaller-Laudel S (2017) Direct
810 isolation of a functional violaxanthin cycle domain from thylakoid membranes of higher plants.
811 Planta 245 (4):793-806.
812 Goss R, Latowski D, Grzyb J, Vieler A, Lohr M, Wilhelm C, Strzalka K (2007) Lipid dependence of
813 diadinoxanthin solubilization and de-epoxidation in artificial membrane systems resembling
814 the lipid composition of the natural thylakoid membrane. BBA-Biomembranes 1768 (1):67-75.
815 Goss R, Lohr M, Latowski D, Grzyb J, Vieler A, Wilhelm C, Strzalka K (2005) Role of hexagonal structure-
816 forming lipids in diadinoxanthin and violaxanthin solubilization and de-epoxidation.
817 Biochemistry 44 (10):4028-4036.
818 Goss R, Nerlich J, Lepetit B, Schaller S, Vieler A, Wilhelm C (2009) The lipid dependence of
819 diadinoxanthin de-epoxidation presents new evidence for a macrodomain organization of the
820 diatom thylakoid membrane. J Plant Physiol 166:1839-1854.
821 Grouneva I, Rokka A, Aro EM (2011) The thylakoid membrane proteome of two marine diatoms
822 outlines both diatom-specific and species-specific features of the photosynthetic machinery. J
823 Proteome Res 10 (12):5338-5353.
824 Guglielmi G, Lavaud J, Rousseau B, Etienne AL, Houmard J, Ruban AV (2005) The light-harvesting
825 antenna of the diatom *Phaeodactylum tricornutum* - Evidence for a diadinoxanthin-binding
826 subcomplex. FEBS J 272 (17):4339-4348.
827 Gugliemelli L (1984) Isolation and characterization of pigment-protein particles from the light-
828 harvesting complex of *Phaeodactylum tricornutum*. Biochimica et Biophysica Acta 766:45-50.
829 Gundermann K, Büchel C (2012) Factors determining the fluorescence yield of fucoxanthin-chlorophyll
830 complexes (FCP) involved in non-photochemical quenching in diatoms. BBA-Bioenergetics
831 1817 (7):1044-1052.
832 Gundermann K, Schmidt M, Weisheit W, Mittag M, Büchel C (2013) Identification of several sub-
833 populations in the pool of light harvesting proteins in the pennate diatom *Phaeodactylum*
834 *tricornutum*. BBA-Bioenergetics 1827 (3):303-310.
835 Gundermann K, Wagner V, Mittag M, Büchel C (2019) Fucoxanthin-chlorophyll protein complexes of
836 the centric diatom *Cyclotella meneghiniana* differ in Lhcx1 and Lhcx6_1 content. Plant Physiol
837 179:779–1795.
838 Guschina IA, Harwood JL (2006) Lipids and lipid metabolism in eukaryotic algae. Prog Lip Res 45 (2):160-
839 186.
840 Herbstová M, Bína D, Kaňa R, Vácha F, Litvín R (2017) Red-light phenotype in a marine diatom involves
841 a specialized oligomeric red-shifted antenna and altered cell morphology. Sci Rep 7 (1):1-10.
842 Herbstová M, Bína D, Koník P, Gardian Z, Vácha F, Litvín R (2015) Molecular basis of chromatic
843 adaptation in pennate diatom *Phaeodactylum tricornutum*. BBA-Bioenergetics 1847 (6–7):534-
844 543.
845 Ikeda Y, Komura M, Watanabe M, Minami C, Koike H, Itoh S, . . . Satoh K (2008) Photosystem I
846 complexes associated with fucoxanthin-chlorophyll-binding proteins from a marine centric
847 diatom, *Chaetoceros gracilis*. BBA-Bioenergetics 1777 (4):351-361.
848 Ikeda Y, Yamagishi A, Komura M, Suzuki T, Dohmae N, Shibata Y, . . . Satoh K (2013) Two types of
849 fucoxanthin-chlorophyll-binding proteins I tightly bound to the photosystem I core complex in
850 marine centric diatoms. BBA-Bioenergetics 1827:529-539.

851 Joshi-Deo J, Schmidt M, Gruber A, Weisheit W, Mittag M, Kroth PG, Büchel C (2010) Characterization
852 of a trimeric light-harvesting complex in the diatom *Phaeodactylum tricornutum* built of FcpA
853 and FcpE proteins. J Exp Bot 61:3079-3087.
854 Juhas M, Büchel C (2012) Properties of photosystem I antenna protein complexes of the diatom
855 *Cyclotella meneghiniana*. J Exp Bot 63:3673-3681.
856 Kalaji HM, Schansker G, Ladle RJ, Goltsev V, Bosa K, Allakhverdiev SI, . . . Zivcak M (2014) Frequently
857 asked questions about in vivo chlorophyll fluorescence: practical issues. Photosynth Res 122
858 (2):121-158.
859 Kansy M, Volke D, Sturm L, Wilhelm C, Hoffmann R, Goss R (2020) Pre-purification of diatom pigment
860 protein complexes provides insight into the heterogeneity of FCP complexes. BMC Plant Biol
861 20 (1):456. doi:10.1186/s12870-020-02668-x.
862 Kern J, Guskov A (2011) Lipids in photosystem II: Multifunctional cofactors. J Photochem Photobiol B
863 104 (1):19-34.
864 Kirchhoff H (2014) Diffusion of molecules and macromolecules in thylakoid membranes. BBA-
865 Bioenergetics 1837 (4):495-502.
866 Kirchhoff H, Hall C, Wood M, Herbstová M, Tsabari O, Nevo R, . . . Reich Z (2011) Dynamic control of
867 protein diffusion within the granal thylakoid lumen. Proc Natl Acad Sci USA 108 (50):20248.
868 Kirchhoff H, Schöttler MA, Maurer J, Weis E (2004) Plastocyanin redox kinetics in spinach chloroplasts:
869 evidence for disequilibrium in the high potential chain. BBA-Bioenergetics 1659 (1):63-72.
870 Kraay GW, Zapata M, Veldhuis MJW (1992) Separation of chlorophylls c1, c2, and c3 of marine
871 phytoplancton by reversed-phase-C18-high-performance liquid chromatography. J Phycol
872 28:708-712.
873 Krüger TP, Malý P, Alexandre MT, Mančal T, Büchel C, Van Grondelle R (2017) How reduced excitonic
874 coupling enhances light harvesting in the main photosynthetic antennae of diatoms. Proc Natl
875 Acad Sci USA 114 (52):E11063-E11071.
876 Kühlbrandt W, Wang DN, Fujiyoshi Y (1994) Atomic model of plant light-harvesting complex by electron
877 crystallography. Nature 367 (6464):614-621.
878 Latowski D, Akerlund HE, Strzalka K (2004) Violaxanthin de-epoxidase, the xanthophyll cycle enzyme,
879 requires lipid inverted hexagonal structures for its activity. Biochemistry 43 (15):4417-4420.
880 Latowski D, Kruk J, Burda K, Skrzynecka-Jaskier M, Kostecka-Gugala A, Strzalka K (2002) Kinetics of
881 violaxanthin de-epoxidation by violaxanthin de-epoxidase, a xanthophyll cycle enzyme, is
882 regulated by membrane fluidity in model lipid bilayers. Eur J Biochem 269 (18):4656-4665.
883 Lavaud J, Rousseau B, Etienne AL (2003) Enrichment of the light-harvesting complex in diadinoxanthin
884 and implications for the nonphotochemical fluorescence quenching in diatoms. Biochemistry
885 42 (19):5802-5808.
886 Lepetit B, Goss R, Jakob T, Wilhelm C (2012) Molecular dynamics of the diatom thylakoid membrane
887 under different light conditions. Photosynth Res 111 (1-2):245-257.
888 Lepetit B, Volke D, Gilbert M, Wilhelm C, Goss R (2010) Evidence for the existence of one antenna-
889 associated, lipid-dissolved, and two protein-bound pools of diadinoxanthin cycle pigments in
890 diatoms. Plant Physiol 154:1905-1920.
891 Lepetit B, Volke D, Szabo M, Hoffmann R, Garab GZ, Wilhelm C, Goss R (2007) Spectroscopic and
892 molecular characterization of the oligomeric antenna of the diatom *Phaeodactylum*
893 *tricornutum*. Biochemistry 46 (34):9813-9822.
894 Levitan O, Chen M, Kuang X, Cheong KY, Jiang J, Banal M, . . . Dai W (2019) Structural and functional
895 analyses of photosystem II in the marine diatom *Phaeodactylum tricornutum*. Proc Natl Acad
896 Sci USA 116 (35):17316.
897 Lohr M, Wilhelm C (1999) Algae displaying the diadinoxanthin cycle also possess the violaxanthin cycle.
898 Proc Natl Acad Sci USA 96 (15):8784-8789
899 Liu ZF, Yan HC, Wang KB, Kuang TY, Zhang JP, Gui LL, . . . Chang WR (2004) Crystal structure of spinach
900 major light-harvesting complex at 2.72 angstrom resolution. Nature 428 (6980):287-292.
901 Mann DG, Vanormelingen P (2013) An inordinate fondness? The number, distributions, and origins of
902 diatom species. J Eukaryot Microbiol 60 (4):414-420.

Mock T, Kroon BMA (2002) Photosynthetic energy conversion under extreme conditions - I: important role of lipids as structural modulators and energy sink under N-limited growth in Antarctic sea ice diatoms. Phytochemistry 61 (1):41-51.

Murata N, Siegenthaler P-A (1998) Lipids in photosynthesis: an overview. In: Siegenthaler PA MN (ed) Lipids in photosynthesis: structure, function and genetics. Kluwer Academic Publishers, Dordrecht, pp 1-20

Nagao R, Kato K, Ifuku K, Suzuki T, Kumazawa M, Uchiyama I, . . . Akita F (2020) Structural basis for assembly and function of a diatom photosystem I-light-harvesting supercomplex. Nat Commun 11 (1):2481.

Nagao R, Kato K, Suzuki T, Ifuku K, Uchiyama I, Kashino Y, . . . Akita F (2019a) Structural basis for energy harvesting and dissipation in a diatom PSII–FCPII supercomplex. Nat Plants 5 (8):890-901.

Nagao R, Takahashi S, Suzuki T, Dohmae N, Nakazato K, Tomo T (2013a) Comparison of oligomeric states and polypeptide compositions of fucoxanthin chlorophyll a/c-binding protein complexes among various diatom species. Photosynth Res 117 (1-3):281-288.

Nagao R, Tomo T, Noguchi E, Suzuki T, Okumura A, Narikawa R, . . . Ikeuchi M (2012) Proteases are associated with a minor fucoxanthin chlorophyll a/c-binding protein from the diatom, *Chaetoceros gracilis*. BBA-Bioenergetics 1817 (12):2110-2117.

Nagao R, Ueno Y, Akita F, Suzuki T, Dohmae N, Akimoto S, Shen J-R (2019b) Biochemical characterization of photosystem I complexes having different subunit compositions of fucoxanthin chlorophyll a/c-binding proteins in the diatom *Chaetoceros gracilis*. Photosynth Res 140 (2):141-149.

Nagao R, Yokono M, Akimoto S, Tomo T (2013b) High excitation energy quenching in fucoxanthin chlorophyll a/c-binding protein complexes from the diatom *Chaetoceros gracilis*. J Phys Chem B 117:6888–6895.

Nagao R, Yokono M, Ueno Y, Shen J-R, Akimoto S (2018) Low-energy chlorophylls in fucoxanthin chlorophyll a/c-binding protein conduct excitation energy transfer to photosystem I in diatoms. J Phys Chem B 123 (1):66-70.

Neilson JA, Durnford DG (2010) Structural and functional diversification of the light-harvesting complexes in photosynthetic eukaryotes. Photosynth Res 106 (1-2):57-71.

Novoderezhkin VI, Palacios MA, Van Amerongen H, Van Grondelle R (2004) Energy-transfer dynamics in the LHCII complex of higher plants: modified redfield approach. J Phys Chem B 108 (29):10363-10375.

Nymark M, Grønbech Hafskjold MC, Volpe C, Fonseca DdM, Sharma A, Tsirvouli E, . . . Bones AM (2021) Functional studies of CpSRP54 in diatoms show that the mechanism of thylakoid protein insertion differs from that in plants and green algae. Plant J 106 (1):113-132.

Nymark M, Valle KC, Brembu T, Hancke K, Winge P, Andresen K, . . . Bones AM (2009) An integrated analysis of molecular acclimation to high light in the marine diatom *Phaeodactylum tricornutum*. PLoS One 4 (11):e7743.

Nymark M, Volpe C, Hafskjold MCG, Kirst H, Serif M, Vadstein O, . . . Winge P (2019) Loss of ALBINO3b insertase results in truncated light-harvesting antenna in diatoms. Plant Physiol 181 (3):1257-1276.

Oka K, Ueno Y, Yokono M, Shen J-R, Nagao R, Akimoto S (2020) Adaptation of light-harvesting and energy-transfer processes of a diatom *Phaeodactylum tricornutum* to different light qualities. Photosynth Res https://doi.org/10.1007/s11120-020-00714-1.

Owens T (1988) Light-harvesting antenna systems in the chlorophyll a/c-containing algae. In: Stevens SE BD (ed) Light-energy transduction in photosynthesis: higher plants and bacterial models. . Rockville, Maryland, pp 122-136

Owens TG, World ER (1986) Light-harvesting function in the diatom *Phaeodactylum tricornutum*: I. Isolation and characterization of pigment-protein-complexes. Plant Physiol 80:732-738.

Papagiannakis E, van Stokkum IHM, Fey H, Büchel C, van Grondelle R (2005) Spectroscopic characterization of the excitation energy transfer in the fucoxanthin-chlorophyll protein of diatoms. Photosynth Res 86 (1-2):241-250.

955 Pi X, Zhao S, Wang W, Liu D, Xu C, Han G, . . . Shen J-R (2019) The pigment-protein network of a diatom
956 photosystem II-light-harvesting antenna supercomplex. Science 365:eaax4406.
957 Premvardhan L, Bordes L, Beer A, Büchel C, Robert B (2009) Carotenoid structures and environments
958 in trimeric and oligomeric fucoxanthin chlorophyll a/c proteins from Resonance Raman
959 Spectroscopy. J Phys Chem B 113 (37):12565-12574.
960 Premvardhan L, Papagiannakis E, Hiller RG, Van Grondelle R (2005) The charge-transfer character of
961 the S0→ S2 transition in the carotenoid peridinin is revealed by Stark spectroscopy. J Phys
962 Chem B 109 (32):15589-15597.
963 Premvardhan L, Robert B, Beer A, Buchel C (2010) Pigment organization in fucoxanthin chlorophyll
964 a/c(2) proteins (FCP) based on resonance Raman spectroscopy and sequence analysis. BBA-
965 Bioenergetics 1797 (8):1647-1656.
966 Premvardhan L, Sandberg DJ, Fey H, Birge RR, Büchel C, van Grondelle R (2008) The charge-transfer
967 properties of the S state of fucoxanthin in solution and in fucoxanthin chlorophyll-a/c protein
968 (FCP) based on stark spectroscopy and molecular-orbital theory. J Phys Chem B 112
969 (37):11838-11853.
970 Pyszniak AM, Gibbs SP (1992) Immunocytochemical localization of photosystem I and the fucoxanthin-
971 chlorophyll-a/c light-harvesting complex in the diatom *Phaeodactylum tricornutum*.
972 Protoplasma 166 (3-4):208-217.
973 Röding A, Boekema E, Büchel C (2018) The structure of FCPb, a light-harvesting complex in the diatom
974 *Cyclotella meneghiniana*. Photosynth Res 135 (1-3):203-211.
975 Rousch JM, Bingham SE, Sommerfeld MR (2003) Changes in fatty acid profiles of thermo-intolerant and
976 thermo-tolerant marine diatoms during temperature stress. J Exp Mar Biol Ecol 295 (2):145-
977 156.
978 Schaller-Laudel S, Latowski D, Jemiola-Rzeminska M, Strzalka K, Daum S, Bacia K, . . . Goss R (2017)
979 Influence of thylakoid membrane lipids on the structure of aggregated light-harvesting
980 complexes of the diatom *Thalassiosira pseudonana* and the green alga *Mantoniella squamata*.
981 Physiol Plant 160 (3):339-358.
982 Schaller S, Latowski D, Jemiola-Rzeminska M, Wilhelm C, Strzalka K, Goss R (2010) The main thylakoid
983 membrane lipid monogalactosyldiacylglycerol (MGDG) promotes the de-epoxidation of
984 violaxanthin associated with the light-harvesting complex of photosystem II (LHCII). BBA-
985 Bioenergetics 1797 (3):414-424.
986 Schober AF, Rio Bartulos C, Bischoff A, Lepetit B, Gruber A, Kroth PG (2019) Organelle studies and
987 proteome analyses of mitochondria and plastids fractions from the diatom *Thalassiosira*
988 *pseudonana*. Plant Cell Physiol 60 (8):1811-1828.
989 Singer SJ, Nicolson GL (1972) The Fluid Mosaic Model of the Structure of Cell Membranes. Science 175
990 (4023):720.
991 Smith BM, Melis A (1988) Photochemical apparatus organization in the diatom *Cylindrotheca*
992 *fusiformis*: Photosystem stoichiometry and excitation distribution in cells grown under high
993 and low irradiance. Plant Cell Physiol 29:761-769.
994 Songaila E, Augulis Rn, Gelzinis A, Butkus V, Gall A, Büchel C, . . . Valkunas L (2013) Ultrafast energy
995 transfer from chlorophyll c 2 to chlorophyll a in fucoxanthin–chlorophyll protein complex. J
996 Phys Chem Lett 4 (21):3590-3595.
997 Standfuss J, van Scheltinga ACT, Lamborghini M, Kühlbrandt W (2005) Mechanisms of photoprotection
998 and nonphotochemical quenching in pea light-harvesting complex at 2.5A resolution. EMBO J
999 24 (5):919-928.
1000 Strzepek RF, Harrison PJ (2004) Photosynthetic architecture differs in coastal and oceanic diatoms.
1001 Nature 431 (7009):689-692.
1002 Szábo M, Lepetit B, Goss R, Wilhelm C, Mustardy L, Garab G (2008) Structurally flexible macro-
1003 organization of the pigment-protein complexes of the diatom *Phaeodactylum tricornutum*.
1004 Photosynth Res 95 (2-3):237-245.
1005 Szábo M, Premvardhan L, Lepetit B, Goss R, Wilhelm C, Garab G (2010) Functional heterogeneity of the
1006 fucoxanthins and fucoxanthin-chlorophyll proteins in diatom cells revealed by their

electrochromic response and fluorescence and linear dichroism spectra. Chem Phys 373:110-114.
Taddei L, Chukhutsina V, Lepetit B, Stella GR, Bassi R, van Amerongen H, . . . Falciatore A (2018) Dynamic changes between two LHCX-related energy quenching sites control diatom photoacclimation. Plant Physiol 177:953-965.
Thamatrakoln K, Bailleul B, Brown CM, Gorbunov MY, Kustka AB, Frada M, . . . Bidle KD (2013) Death-specific protein in a marine diatom regulates photosynthetic responses to iron and light availability. Proc Natl Acad Sci USA 110 (50):20123-20128.
Vaswani HM, Hsu C-P, Head-Gordon M, Fleming GR (2003) Quantum chemical evidence for an intramolecular charge-transfer state in the carotenoid peridinin of peridinin− chlorophyll− protein. J Phys Chem B 107 (31):7940-7946.
Veith T, Brauns J, Weisheit W, Mittag M, Büchel C (2009) Identification of a specific fucoxanthin-chlorophyll protein in the light harvesting complex of photosystem I in the diatom *Cyclotella meneghiniana*. BBA-Bioenergetics 1787 (7):905-912.
Veith T, Büchel C (2007) The monomeric photosystem I-complex of the diatom *Phaeodactylum tricornutum* binds specific fucoxanthin chlorophyll proteins (FCPs) as light-harvesting complexes. BBA-Bioenergetics 1767 (12):1428-1435.
Vieler A, Wilhelm C, Goss R, Sub R, Schiller J (2007) The lipid composition of the unicellular green alga *Chlamydomonas reinhardtii* and the diatom *Cyclotella meneghiniana* investigated by MALDI-TOF MS and TLC. Chem Phys Lipids 150 (2):143-155.
Wang W, Yu L-J, Xu C, Tomizaki T, Zhao S, Umena Y, . . . Suga MJS (2019) Structural basis for blue-green light harvesting and energy dissipation in diatoms. Science 363 (6427):eaav0365.
Wang W, Zhao S, Pi X, Kuang T, Sui S-F, Shen J-R (2020) Structural features of the diatom photosystem II–light-harvesting antenna complex. FEBS J 287:2191–2200.
West RG, Bína D, Fuciman M, Kuznetsova V, Litvín R, Polívka T (2018) Ultrafast multi-pulse transient absorption spectroscopy of fucoxanthin chlorophyll a protein from *Phaeodactylum tricornutum*. BBA-Bioenergetics 1859 (5):357-365.
Wilhelm C, Goss R, Garab G (2020) The fluid-mosaic membrane theory in the context of photosynthetic membranes: Is the thylakoid membrane more like a mixed crystal or like a fluid? J Plant Physiol 252:153246.
Xu C, Pi X, Huang Y, Han G, Chen X, Qin X, . . . Shen JR (2020) Structural basis for energy transfer in a huge diatom PSI-FCPI supercomplex. Nat Commun 11 (1):5081.
Yan X, Chen D, Xu J, Zhou C (2011) Profiles of photosynthetic glycerolipids in three strains of *Skeletonema* determined by UPLC-Q-TOF-MS. J Appl Phycol 23 (2):271-282.
Yongmanitchai W, Ward OP (1993) Positional distribution of fatty acids, and molecular species of polar lipids, in the diatom *Phaeodactylum tricornutum*. J Gen Microbiol 139 (3):465-472.
Zhu SH, Green BR (2010) Photoprotection in the diatom *Thalassiosira pseudonana*: Role of LI818-like proteins in response to high light stress. BBA-Bioenergetics 1797 (8):1449-1457.
Zigmantas D, Hiller RG, Sharples FP, Frank HA, Sundström V, Polívka T (2004) Effect of a conjugated carbonyl group on the photophysical properties of carotenoids. Phys Chem Chem Phys 6 (11):3009-3016.

Acknowledgements

BB acknowledges financial support from the European Research Council (ERC) under the European Union Horizon 2020 research and innovation program (grant agreement no. 715579). BL thanks the Deutsche Forschungsgemeinschaft (LE3358/3-2) and the Baden-Württemberg Stiftung (Elite program) for financial support. CB acknowledges support by the European Union's Horizon 2020 research and innovation programme under the Marie Skłodowska-Curie grant agreement No 675006 and from the Deutsche Forschungsgemeinschaft, grant Bu 812 10-1. DAC thanks the Canada Research Chairs and Natural Science and Engineering Research Council of Canada for support. JL thanks the Centre National de la Recherche Scientifique-CNRS, the Natural Sciences and Engineering Research Council of Canada-NSERC (Discovery and Northern Supplement grants), the Canada First Research Excellence Fund-Sentinelle Nord, and the strategic research cluster Québec-Océan for their financial support. All authors thank the reviewer for valuable suggestions.